Quantum internal modes of solitons in a one-dimensional easy-plane antiferromagnet in a strong magnetic field

B. A. Ivanov and A. K. Kolezhuk
Institute of Magnetism, National Academy of Sciences and Ministry of Education of Ukraine, 36 Vernadskii av., 252142 Kiev, Ukraine
(Received 12 February 1997; revised manuscript received 5 May 1997)

We use the effective Lagrangian approach to study the dynamics of solitons in a one-dimensional easy-plane Heisenberg antiferromagnet in the presence of a strong external in-plane magnetic field H close to a certain critical value $H_c \simeq (H_e H_a)^{1/2}$ (where H_e and H_a are the exchange and anisotropy fields, respectively). We show that the dynamics of internal soliton degrees of freedom is essentially quantum, and they are strongly coupled to the ''translational'' mode of soliton movement. These peculiarities lead to considerable changes in the response functions of the system that can be detected experimentally; we discuss the possibility to observe the signatures of internal soliton modes in $(CD_3)_4NMnCl_3$ (TMMC). [S0163-1829(97)04638-9]

I. INTRODUCTION

Study of soliton excitations in one-dimensional (1D) systems have been attracting much attention since the pioneering work by Krumhansl and Schrieffer.[1] Mikeska[2] was the first to calculate the contribution of solitons into observable quantities for the realistic system, viz. the quasi-1D easy-plane ferromagnet $CsNiF_3$ in an external magnetic field. His prediction of the soliton-induced central peak in the dynamical structure factor was confirmed experimentally,[3] which gave rise to intensive theoretical and experimental studies. Since then, soliton signatures were reliably observed in static and dynamic characteristics of various 1D magnets with both ferromagnetic and antiferromagnetic coupling, see recent reviews.[4,5]

The easy-plane 1D antiferromagnetic compound TMMC $[(CD_3)_4NMnCl_3]$ in an external field is one of the most widely studied materials[6–14] (see also Ref. 4 and references therein). Its magnetic ions have spin $S=5/2$, and thus it is believed that the dynamics of TMMC can be well described on the basis of classical equations of motion for the sublattice magnetization. It is well known that in the presence of a strong magnetic field the equations of motion for antiferromagnets are rather complicated and cannot be reduced to the sine-Gordon (SG) model because of the importance of out-of-plane deviations.[9,13] Effective field-induced anisotropy competes with the easy-plane anisotropy, so that at a certain critical field $H_c \simeq (H_e H_a)^{1/2}$ (where H_e and H_a are the exchange and anisotropy fields, respectively) in-plane and out-of-plane magnon modes have equal excitation energies, and the SG approximation becomes obviously inadequate for H close to H_c.

At $H=H_c$ the ''easy plane'' effectively changes. There are, respectively, two types of static kink solutions,[8] one of which has lower energy at $H<H_c$ and the other at $H>H_c$. Corresponding dynamic solutions are much less understood. Different authors[9,13,15–17] obtained contradictory results concerning their stability. It was shown[13,16,17] that the effective plane of rotation of the sublattice magnetization in a kink depends on the kink velocity, and the two types of kinks transform into each other at some critical velocity v_c, $v_c \to 0$ at $H \to H_c$.

The main feature of the problem, determining kink stability and dynamics in strong magnetic fields, is the presence of an out-of plane magnon mode localized at the kink.[16,17,5] This internal mode is highly nonlinear at $v \to v_c$ and strongly coupled to the ''translational'' (zero) mode of the kink motion,[5] which makes its analysis rather complicated. Moreover, it can be shown that because of the relatively small effective mass of solitons [the ratio of soliton and magnon masses is S for antiferromagnets, while for ferromagnets this ratio is proportional to the large parameter $S(H_e/H_a)^{1/2}$] the dynamics of internal soliton degrees of freedom in antiferromagnets is essentially quantum even for ''almost classical'' values of S such as 5/2 (Refs. 5 and 18) and exhibits subtle effects distinguishing between integer and half-integer S.[19,20] Thus, in our opinion, the internal dynamics of solitons in TMMC in a strong-field regime can be highly nontrivial, and its consistent description, as well as experimental observation, is a fascinating problem.

In this paper we present a detailed theoretical study of the soliton dynamics in a 1D ''almost-classical'' spin-S easy-plane antiferromagnet in a strong external magnetic field close to the critical value H_c. We use the effective Lagrangian approach (valid for H close to H_c) to reduce approximately the original field problem to one with a finite number of degrees of freedom, and after that a common canonical quantization is performed. We show that quantum effects (tunneling between two energetically equivalent kink states) lead to the appearance of a localized mode that is also coupled to the translational mode and thus depends on the soliton momentum P. At $P=0$ the tunneling is suppressed for half-integer S due to the topological effects, but at nonzero P it becomes possible for any S. We calculate the contribution of the localized modes into the dynamic structure factor (DSF) and show that it leads to an additional peak concentrated at nonzero frequency, which can be detected by electron spin resonance (ESR) or inelastic neutron scattering (INS) technique. Numerical estimations of the corresponding resonance frequencies and the peak properties for TMMC are given. To our knowledge, at present the only known experiment probing internal soliton modes is the so-called ''soliton magnetic resonance'' [21] in the Ising-type quasi-1D antiferro-

magnet $CsCoCl_3$, and no such data exist for the Heisenberg magnets.

This paper is organized as follows: In Sec. II we introduce the model. In Sec. III we derive an effective model of internal kink dynamics, perform classical linear analysis of the spectrum of excitations against the background of kinks, and discuss the soliton stability problem, and in Sec. IV we perform quantization of the effective model and discuss the behavior of the energy levels of localized modes. In Sec. V the soliton contribution to the response functions is considered, and numerical estimations of predicted effects for TMMC are given. Finally, Sec. VI contains concluding remarks.

II. MODEL

We consider a one-dimensional two-sublattice Heisenberg antiferromagnet (AFM) of the TMMC type in an external magnetic field. This system is well described by the following Hamiltonian:

$$\mathcal{H}=\sum_n \{J\vec{S}_n\vec{S}_{n+1}+D_1(S_n^z)^2-D_2(S_n^y)^2-g\mu_B\vec{H}\vec{S}_n\}, \quad (1)$$

where $J>0$ is the exchange constant, μ_B is the Bohr magneton, g is the Landé factor, D_1 and D_2 are anisotropy constants, $D_1 \gg D_2 > 0$, $\vec{H}$ is the magnetic field, and spins $\vec{S}_n$ are treated as classical vectors. In the absence of the field xy is an easy plane, and y is the easiest axis in this plane (the case of ''pure'' easy-plane AFM corresponds to $D_2=0$); the chain axis is along z. For TMMC the value of the spin is $S=\frac{5}{2}$, and the following values for the parameters of the classical Hamiltonian have been established:[10] $JS^2=85$ K, $D_1S^2=1.9$ K, $D_2S^2=0.022$ K, and $g=2.01$.

Long-wavelength dynamics of AFM can be described within the nonlinear sigma model approach. It is convenient to introduce the antiferromagnetism vector (the sublattice magnetization) $\vec{l}_i=(\vec{S}_{2i+1}-\vec{S}_{2i})/2S$ at each magnetic elementary cell. At low temperatures, when the magnetization $\vec{m}_i=(\vec{S}_{2i+1}+\vec{S}_{2i})/2S$ is small, $\vec{l}$ can be regarded as a unit vector, and after passing to the continuum limit the following Lagrangian can be obtained:

$$L=\frac{1}{2}JS^2a\int dz\left\{\frac{1}{c^2}(\partial_t\vec{l})^2-(\partial_z\vec{l})^2-\frac{1}{x_0^2}l_z^2-\frac{1}{x_b^2}-\frac{\gamma^2}{c^2}(\vec{l}\cdot\vec{H})^2+\frac{2\gamma}{c^2}\vec{H}\cdot(\vec{l}\times\partial_t\vec{l})\right\}+\frac{\hbar S}{2}\int dz\,\vec{l}\cdot(\nabla\vec{l}\times\partial_t\vec{l}). \quad (2)$$

One can find derivation from different points of view in Refs. 22–25; this approach is closely related to the commonly used Mikeska's formulation.[6] Here a is the lattice spacing, $c=2JSa/\hbar$ is the limiting velocity of spin waves, $\gamma=g\mu_{B/\hbar}$ is the gyromagnetic ratio, and $x_0=a[J/2(D_1+D_2)]^{1/2}$ and $x_b=a(J/2D_2)^{1/2}$ are the characteristic length scales. The last term in Eq. (2) is the so-called topological term, which can be rewritten as $2\pi\hbar SQ$, where Q is the Pontryagin index (the winding number) of a given space-time configuration of the field $\vec{l}$. This term is irrelevant in classical analysis, but is very important for the quantum theory since it distinguishes between integer and half-integer S.

Within this approximation, the vector of magnetization $\vec{m}$ is a ''slave'' variable and can be expressed through the antiferromagnetism vector $\vec{l}$:

$$\vec{m}=\frac{\hbar}{4JS}(\vec{l}\times\partial_t\vec{l})+\frac{g\mu_B}{4J}\{\vec{H}-\vec{l}(\vec{H}\cdot\vec{l})\}-\frac{1}{2}a\nabla\vec{l}. \quad (3)$$

Further, it is convenient to introduce angular variables for the vector $\vec{l}$. We choose the easiest axis y as a polar one, and put

$$l_y=\cos\theta, \quad l_z=\sin\theta\cos\varphi, \quad l_x=\sin\theta\sin\varphi.$$

Let us set the field in plane perpendicular to the easy axis, $\vec{H}\|\hat{\vec{x}}$, then y is always the easiest axis, and there is no spin-flop transition. However, at $H=H_c$, where

$$H_c=2(2JD_1S^2)^{1/2}, \quad (4)$$

the axes x and z switch their roles: the easy plane is xy when $H<H_c$, and yz when $H>H_c$. In this paper, we consider the case of strong fields $H\approx H_c$; for TMMC the critical field is of the order of 100 kOe. In what follows, we can safely neglect any contribution coming from D_2 because in strong fields the field-induced anisotropy in the basal plane is much larger than the initial crystal-field anisotropy. Hereafter, we assume that the field is close to H_c, and regard the quantity

$$\rho=1-(H/H_c)^2 \quad (5)$$

as a small parameter playing the role of effective rhombicity (as far as only static properties are considered, $H=H_c$ corresponds to a ''uniaxial'' situation).

III. EFFECTIVE MODEL OF KINK DYNAMICS

Because of the presence of magnetic field, the equations of motion for the model (2) contain not only the usual Lorentz-invariant terms, but also terms of the first order in time derivatives, and thus their analysis is rather complicated. However, one can easily find static soliton solutions. There are two types of static kinks, with $\vec{l}$ rotating in the xy plane ($\varphi=\pm\pi/2$) or in the yz plane ($\varphi=0,\pi$).[8] The behavior of the angle θ in both kinks is given by

$$\cos\theta_0=\pm\tanh[(z-z_s)/z_0], \quad (6)$$

where the kink thickness is $z_0=x_0$ for the yz kink and $z_0\simeq x_0H_c/H=x_0/(1-\rho)^{1/2}$ for the xy kink, and z_s is an (arbitrary) kink coordinate. For $H<H_c$ the kink with $\varphi=\pm\pi/2$ is the lowest-energy nonlinear excitation, and for $H>H_c$ this role goes to the kink with $\varphi=0,\pi$; at $H=H_c$ their energies are equal, as well as the energies of in-plane and out-of-plane magnon branches.

As shown in Refs. 26 and 16, approximate soliton solutions can be constructed using the following trick: from the equations of motion determined by the Lagrangian (2) one can easily see that the characteristic space scale of the φ variation $l_\varphi=x_0/\sqrt{\rho}$ is much larger than the characteristic thickness of the kink x_0. Then, ''within the kink,'' i.e.,

within the region where the variation of θ mainly takes place, we can neglect the spatial dependence of φ and put $\varphi=\varphi_s=\text{const}$. Such approximate soliton solutions with constant φ, as shown in Refs. 26 and 16, can be obtained for arbitrary velocity, and the only requirement is that ρ has to be small. The angle of out-of-plane deviation φ_s changes from $\pm\pi/2$ to $0,\pi$ when the velocity changes from 0 to a certain critical value.

To study the dynamics of out-of-plane motion, we use the same trick, but regard z_s and φ_s as new dynamic variables slowly varying in time: we assume that the soliton solution has the form

$$\cos\theta_s=\sigma\ \tanh\left(\frac{z-z_s(t)}{z_0(\varphi_s)}\right),\quad \varphi=\varphi_s(t),$$
$$z_0(\varphi)\equiv x_0(1-\rho\ \sin^2\varphi)^{-1/2}, \tag{7}$$

here $\sigma=\pm1$ is the topological charge distinguishing kinks and antikinks. Substituting the ansatz (7) into the Lagrangian (2) and assuming that z_s and φ_s are ''slow'' variables, i.e.,

$$\dot z_s\ll c,\quad \dot\varphi_s\ll\omega_0\equiv c/x_0, \tag{8}$$

one can obtain the following effective Lagrangian with only two degrees of freedom:

$$L_{\text{eff}}=-E_0(1-\rho\ \sin^2\varphi_s)^{1/2}+\frac{E_0}{2c^2}(\dot z_s^2+x_0^2\dot\varphi_s^2)$$
$$+\frac{\pi E_0}{2c}\sigma\dot z_s(1-\rho)^{1/2}\cos\varphi_s-\hbar S\dot\varphi_s. \tag{9}$$

Here the dot denotes differentiation with respect to time, and $E_0=2S^2(2JD_1)^{1/2}$ is a characteristic energy scale (rest energy of a soliton at $H=H_c$). The last term in the Lagrangian comes from the topological term in Eq. (2) and is ineffective in classical treatment since it is a complete derivative. However, in quantum treatment it changes the definition of canonical momentum conjugate to φ_s, which is very important, as we will see below.

The effective potential for the internal variable φ_s strongly depends on the kink velocity $\dot z_s$. One can see that a classical stability analysis of the effective Lagrangian (9) allows one to reproduce the results of a more rigorous approach of Refs. 16, 17, and 5, which we briefly revisit below. The canonical momentum P conjugate to z_s,

$$P=\frac{E_0}{c^2}\,\dot z_s+P_0(1-\rho)^{1/2}\sigma\ \cos\varphi_s,\quad \text{where}\ \ P_0=\frac{\pi E_0}{2c}, \tag{10}$$

is conserved, and thus it is convenient to express everything in terms of P. The effective potential

$$U_{\text{eff}}=E_0(1-\rho\ \sin^2\varphi_s)^{1/2}$$
$$+\frac{\pi^2E_0}{8}\left\{\frac{P}{P_0}-\sigma\ \cos\varphi_s(1-\rho)^{1/2}\right\}^2 \tag{11}$$

has four extrema as a function of φ_s, at $\varphi_s=0,\pi$ and at $\varphi_s=\varphi_{1,2}(P)$, where $\varphi_{1,2}(P)$ are two roots of the equation

$$\cos(\varphi_s)=\sigma P/P_c, \tag{12}$$

$$P_c\simeq P_0\left\{1-\rho\left(\frac12-\frac{4}{\pi^2}\right)\right\}.$$

Extrema at $\varphi_s=0,\pi$ correspond to yz kinks, and extrema at $\varphi_s=\varphi_{1,2}(P)$ correspond to xy type kinks. When the velocity of an xy-type kink is zero, the plane of rotation of the vector $\vec l$ is xy, and this plane smoothly changes to yz when P tends to P_c, so that an xy-type kink smoothly transforms into a yz kink. The frequency of linear oscillations around those extrema is given by

$$\omega_l^2=\omega_0^2f(\rho)\times\begin{cases}\sigma_0\dfrac{P}{P_c}-1 & \text{for}\ \ \varphi_s=0,\pi\\ 1-\dfrac{P^2}{P_c^2} & \text{for}\ \ \varphi_s=\varphi_{1,2}(P)\end{cases}, \tag{13}$$

where

$$\sigma_0=\sigma\ \text{sgn}(\cos\varphi_s),$$
$$f(\rho)\simeq\frac{\pi^2}{4}\left\{1-\frac{\pi^2-4}{\pi^2}\rho\right\}.$$

Thus, xy-type kinks are stable in the entire region $-P_c\leqslant P\leqslant P_c$ where the corresponding solutions (12) have sense. The stability of yz kinks depends on P and on the sign of the quantity $\sigma_0=\text{sgn}(\theta_0'\cos\varphi_s)$: yz kinks with $\sigma_0>0$ are stable at $P>P_c$, and those with $\sigma_0<0$ are stable at $P<-P_c$. For each yz kink there exist two possible ''daughter'' xy-type kinks, corresponding to the two possible solutions $\varphi_{1,2}(P)$, so that the transition from a yz kink to an xy kink when $|P|$ drops below P_c is a spontaneous breaking of symmetry.

The dispersion relation for soliton excitations, i.e., the dependence of their energy E on the momentum P, is schematically shown in Fig. 1 (the curve labeled ''classical''). For $\rho>0$, i.e., $H<H_c$ the minimal energy is reached at $P=0$, while at $\rho<0$ $(H>H_c)$ the minimum is located at $P=P_0$; in both cases the second derivative d^2E/dP^2 is discontinuous at $P=\pm P_c$.

It should be remarked that the effective model (9) was derived under the assumption that the variable φ_s is ''slow,'' and this assumption has to be checked self-consistently at the end. Thus, the expressions (13) make sense only if $\omega_l^2\ll\omega_0^2$. This does not matter, of course, for the classical linear analysis of stability presented above, because the corresponding frequencies are small in the vicinity of the transition, but it indicates that those classical results cannot be used for the adequate description of the internal dynamics.

Indeed, in linear analysis the localized mode frequency is zero at $P=P_c$, which means (i) strong nonlinearity: anharmonic terms have to be taken into account; (ii) the importance of quantum effects: the magnitude of quantum zero-point fluctuations around the classical minima of the effective potential strongly increases when the potential well becomes ''flat.''

IV. QUANTUM INTERNAL MODES

Since the effective model (9) contains only two degrees of freedom, one can easily quantize it in a canonical way. The

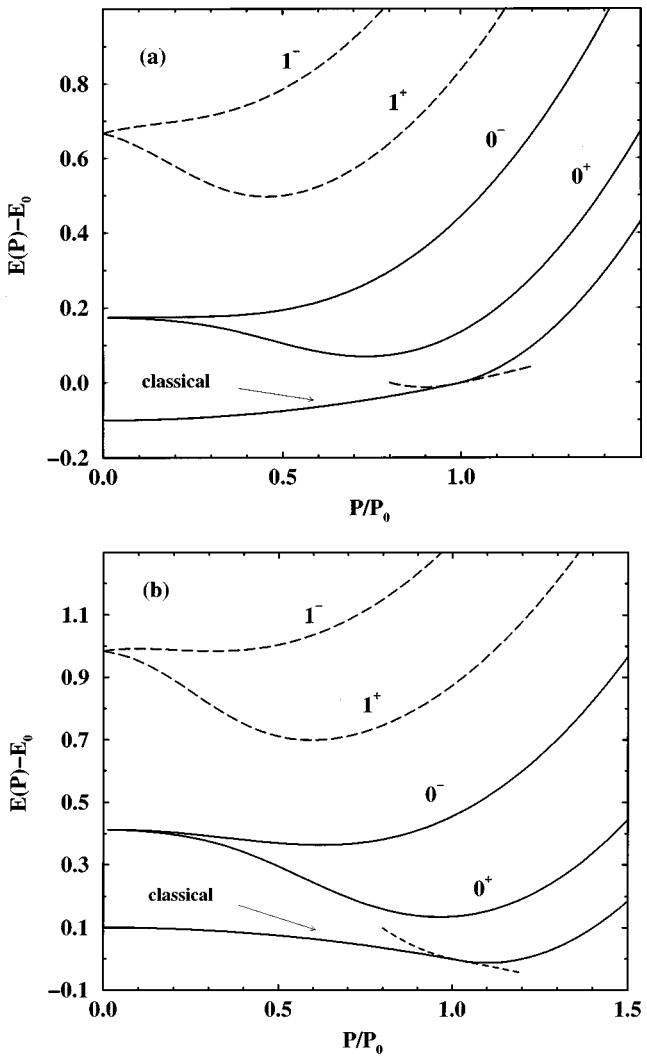

FIG. 1. Typical dependence of the soliton energy levels E on its momentum P for half-integer spin S (levels presented in this figure were computed for $S=\frac{5}{2}$): (a) $H<H_c$ ($\rho=0.2$); (b) $H>H_c$ ($\rho=-0.2$). The curve labeled ''classical'' corresponds to the result of classical calculation (Ref. 5) for the lowest energy state; dashed pieces of the curve indicate unstable states. For $S=\frac{5}{2}$ the $1^{\pm}$ levels are completely inside the magnon continuum and thus are also shown with dashed lines. For integer S the degeneracy at $P=0$ is lifted.

Lagrangian does not depend on z_s and thus the total momentum P is conserved and can be treated as a c number, so that we are left with only one variable φ_s. The Hamiltonian can be easily obtained in the form

$$\hat{H}=\frac{\hbar^2\omega_0^2}{2E_0}\left\{i\frac{\partial}{\partial\varphi_s}+S\right\}^2+U_{\rm eff}(\varphi_s), \tag{14}$$

where S in curly brackets appears because the last term in Eq. (2) changes the definition of the angular momentum. As we will see below, the presence of this term changes the situation drastically depending on whether S is integer or half-integer. For the wave function $\Psi(\varphi_s)$ one has the usual periodic boundary conditions $\Psi(\varphi)=\Psi(\varphi+2\pi)$.

The effective potential $U_{\rm eff}$ generally has two wells, with energetically equivalent well minima; at $P=0$ the minima are located at $\varphi_s=\pm\pi/2$, as P deviates from zero they both move towards 0 or π depending on the sign of P and the ''generalized'' topological charge σ_0, and at $P=\pm P_c$ they merge into one well at $\varphi_s=0$ or π. One may expect that tunneling between equivalent minima at $|P|<P_c$ splits the lowest-energy levels, leading to the appearance of one more internal soliton mode. However, using arguments of the same type as in Refs. 19 and 20, it is easy to show that at $P=0$ the tunneling is possible only for integer S. Indeed, the tunneling amplitude is proportional to the path integral,

$$\int_{\varphi_1(P)}^{\varphi_2(P)}\mathcal{D}\varphi_s\exp\left\{\frac{i}{\hbar}\int dtL_{\rm eff}\right\}, \tag{15}$$

where $\varphi_{1,2}(P)$ are the well minima and the effective Lagrangian is defined by Eq. (9). Since $L_{\rm eff}$ contains the topological term $\hbar S\dot{\varphi}_s$, different paths contribute with the phase factor proportional to $e^{iS\Delta\varphi_s}$, where $\Delta\varphi_s$ is the change in φ_s along the path. At $P=0$ one has two equivalent paths with $\Delta\varphi_s=\pm\pi$, so that their contributions cancel each other for half-integer S (recall that in the case of TMMC $S=\frac{5}{2}$). If $P\neq 0$, the two paths become inequivalent, thus allowing nonzero tunneling amplitude.

The Schrödinger equation with the Hamiltonian (14) can be easily solved numerically, and one gets the energy eigenvalues as functions of the soliton momentum P; a typical level structure is shown in Fig. 1. All states at fixed P,

$$\psi_{n,\nu}(P,\varphi_s)=u_{n,\nu}(P,\varphi_s)e^{iS\varphi_s},$$

can be labeled with two quantum numbers n and ν (ν being the parity of the ''reduced'' wave function u), and for half-integer S odd and even states are degenerate at $P=0$. One can see that quantum effects change the soliton dispersion considerably compared to the classical calculation; particularly, the dispersion tends to have a minimum at nonzero P even for fields lower than H_c, which means that H_c is effectively renormalized towards its decrease. This renormalization is not small, as seen from Fig. 1, since at $\rho=0.2$ the lowest energy is still reached at $P\neq 0$. Unfortunately, we are not able to calculate this renormalization quantitatively: first of all, our effective model is valid only at small ρ and, second, there are other quantum effects influencing the effective soliton energy (the change in the energy of zero-point fluctuations of magnon modes in the presence of a kink) that are not considered here; the interested reader is referred for details to the original papers[27–29] and to the recent review.[4]

From the picture of the energy levels presented in Fig. 1 one can see that there are *two* possible types of out-of-plane modes: one is ''classical'' in the sense that it corresponds to (nonlinear) oscillations of φ around the classical minima in the two-well potential $U_{\rm eff}$; an example of the mode of this type is given by $1^{\pm}$ levels in Fig. 1. The other mode is ''purely quantum;'' it corresponds to tunnelling between two equivalent classical minima and is always the lowest excitation; this mode is unique and is labeled 0^- in Fig. 1.

Again, as in the classical case, the results of semiquantum treatment should be checked for self-consistency at the end: we can trust only in those energy levels that are considerably lower than $E_{\rm g.s.}+\hbar\omega_0$, where $E_{\rm g.s.}$ is the ground-state level (''0^+'' in Fig. 1). From this condition one can see that ''classical'' modes are in fact always ''fast'' and, strictly

speaking, cannot be described adequately within the proposed scheme. Moreover, one can see that actually only one of the ''classical'' modes (namely, ''1^+'') can exist at all, since the energy levels of the other ''classical'' modes are completely inside the magnon continuum and thus they cannot exist as localized modes. The situation, however, is different with the quantum mode: its frequency remains considerably lower than ω_0 in a wide range of P. It is always the lowest excitation and thus the most important one for the low-temperature physics of the system. In this paper, we are mainly interested in this second type of internal excitation, and in the next section we study the possibility of its manifestation in the experimentally observable quantities.

V. INTERNAL SOLITON MODES AND RESPONSE FUNCTIONS

In this section we apply the results obtained so far to find out how the excitation of internal soliton degrees of freedom contributes to the response functions of an easy-plane antiferromagnet in a strong-field regime (H close to H_c).

We wish to begin this section with a remark concerning the relation between the gap in the spectrum of linear excitations $\hbar\omega_0$ and the kink rest energy E_0 in various soliton-bearing systems. For the model of structural phase transition used by Krumhansl and Schrieffer $\hbar\omega_0 \propto \Phi_0$, and $E_0 \propto \Phi_0^3$, where Φ_0 is the magnitude of the order parameter, so that near the transition point $E_0 \ll \hbar\omega_0$, which justifies neglecting kink-phonon interaction at $T \ll E_0$ in Ref. 1. For ferromagnets one obtains $E_0/\hbar\omega_0 \propto S(J/D)^{1/2}$, where J and D are the exchange and anisotropy constants, respectively, so that in the case of the Heisenberg magnets $J/D \gg 1$, and $E_0 \gg \hbar\omega_0$ for any S. For antiferromagnets the situation is ''intermediate'': $E_0/\hbar\omega_0 \propto S$, and the inequality $E_0/\hbar\omega_0 \gg 1$ holds only for $S \gg 1$. One can see that in the large-S limit solitons in antiferromagnets are much ''lighter'' than in ferromagnets; however, for realistic small-S systems the above statement may be true as well: For example, for a 1D easy-plane ferromagnet in an external in-plane magnetic field (the geometry typical for the experiments on widely studied spin-1 quasi-1D compound $CsNiF_3$ with $J=23.6$ K, $D=4.5$ K) the ratio of soliton and magnon energies is $E_0/\hbar\omega_0 = 4S\sqrt{2J/D} \approx 12.95$ for $CsNiF_3$, and for TMMC $E_0/\hbar\omega_0 = S = 5/2$, which is more than five times smaller.

The relation $S \gg 1$ is often used as a condition under which a quantum spin system can be treated classically, but in actual practice the strong inequality is not needed, and classical equations of motion work well, say, for $S=5/2$, as in case of TMMC. Thus, in antiferromagnets for realistic S values E_0 is only a few times greater than $\hbar\omega_0$ (for example, in the case of strong fields close to H_c the characteristic values of the kink energy and magnon gap for TMMC are $E_0 \simeq 20$ K and $\hbar\omega_0 \simeq 7$ K, respectively), and the condition usually used $\hbar\omega_0 \ll T \ll E_0$ can hardly be satisfied as a strong inequality. Therefore, for antiferromagnets $\hbar\omega_0$ is of the order of T within the temperature range $T \ll E_0$ where the phenomenological approach is valid (practically, it is sufficient that $T \lesssim \frac{1}{3} E_0$), so that one should use quantum statistics for magnon modes.

The most general quantity determining the response functions is the so-called dynamical structure factor $S^{\alpha\beta}(q,\omega)$, which is essentially the space-time Fourier component of the two-spin correlation function $\langle S^\alpha(n,t) S^\beta(n',0)\rangle$. In case of antiferromagnet, the quantities of interest are (i) the DSF component at $q=0$, describing the intensity of response in ESR experiments; (ii) the DSF component at $q \approx Q_B$, where Q_B is the Bragg wave vector, which is usually measured in INS experiments. The main contribution to the DSF at $q=Q_B$ comes from the correlator of the antiferromagnetism vector $\langle \vec{l}(z,t)\vec{l}(z',0)\rangle$, and the component at $q=0$ is determined by the correlator of magnetization $\langle \vec{m}(z,t)\vec{m}(z',0)\rangle$.[30] The soliton contribution to the correlation functions can be calculated using the approximation of the soliton ideal gas,[1] which means that at low density of kinks the main role is played by one-soliton correlations. Then one has to deal with correlators of the form

$$\int dz \int dz' e^{iq(z-z')} \langle f(z-z_s(t)) \times A(\varphi_s,t) f(z'-z_s(0)) A(\varphi_s,0)\rangle, \tag{16}$$

where A and f are generally certain operators. The average should be taken in both quantum-mechanical and thermodynamic senses. Quantum-mechanical averaging is performed with the wave functions $\Psi_{\lambda,P} = e^{iPz_s}\psi_\lambda(P,\varphi_s)$ (we use the notation $\lambda=\{n,\nu\}$ for the sake of brevity), and the thermodynamic average should be performed with the Gibbs distribution function

$$w_\lambda(P) = (2\pi\hbar)^{-1} e^{-E_\lambda(P)/T} e^{-\Sigma_s(\lambda,P)/T}, \tag{17}$$

where w is normalized to the total density of solitons, and the quantity Σ_s is the change in the free energy of the magnon gas due to the presence of a kink, which is attributed to the kink in the phenomenological approach:[31]

$$\Sigma_s(\lambda,P) = T\sum_j \int dk \Delta n^{(j)}(k,\lambda,P) \ln[2\sinh(\hbar\omega_k^{(j)}/T)].$$

Here $j=1,2$ labels different branches of magnons of the continuous spectrum, and $\omega_k^{(j)}$ are the frequencies of corresponding modes. The change in the magnon density of states $\Delta n^{(j)}(k,\lambda,P)$ is connected with the phase shift $\Delta_s^{(j)} \times (k,\lambda,P)$ acquired by a magnon of the jth branch with wave vector k after its interaction with the kink having quantum numbers λ, P: $\Delta n^{(j)} = (1/2\pi)(d\Delta_s^{(j)}/dk)$. [In fact, Σ_s contains divergent terms connected with the change in the energy of zero-point vibrations between the ground state and the one-soliton state. This divergence, however, is compensated by the counterterms arising from the normal ordering of operators, yielding finite quantum correction to the soliton energy.[27–29]]

Using the above arguments, expression (16) can be rewritten as

$$|f(q)|^2 \sum_{\lambda,\lambda'} \int dP e^{-[E_\lambda(P)+\Sigma_s(\lambda,P)]/T} \times |\langle \lambda,P|\hat{A}|\lambda',P-\hbar q\rangle|^2 \delta(E_\lambda(P) - E_{\lambda'}(P-\hbar q) - \hbar\omega), \tag{18}$$

where $|\lambda,P\rangle \equiv \psi_\lambda(P)$. At low temperatures $T \ll E_0$ one may take into account only the contribution of the lowest two soliton levels $0^\pm$ (see Fig. 1).

At $T \ll \hbar\omega_0$, Σ_s is proportional to $\exp(-\hbar\omega_0/T)$ and can be neglected. At $T \gg \hbar\omega_0$ the effect of Σ_s becomes significant; its accurate calculation requires solving the soliton-magnon scattering problem to get the phase shifts, which is too complicated to do analytically. However, zy-type solitons, i.e., kinks with $P \geqslant P_c$, classically have $\varphi_s = 0, \pi$, thus being ''sine-Gordon'' in structure, and the phase shifts for the sine-Gordon problem are known. In this case $\Delta_s^{(1,2)}(k) \simeq -2\arctan(kx_0)$ at small kink velocities $v \ll c$, and for $T \gg \hbar\omega_0$ we obtain the well-known SG result

$$\Sigma_s = -2T\ \ln 2 - 2T\ \ln(\hbar\omega_0/T).$$

On the other hand, the same SG result should be valid for xy solitons with $P=0$. We will assume that the same expression can be applied for all P; this assumption seems plausible though it cannot be justified in a rigorous way. One can expect that the possible weak dependence of Σ_s will lead to certain renormalization of the P dependence of the soliton energy levels E_λ, but we believe that our results will remain qualitatively correct.

The conditions necessary for the consistency of our approach to calculate the response functions can be summarized as follows: (i) smallness of ρ; (ii) smallness of the temperature T (compared with the soliton energy E_0 or, better, compared with the magnon energy $\hbar\omega_0$ to avoid the possible influence of the P dependence of unknown phase shifts as described above); (iii) only the low-frequency part (at most up to $\Omega = \omega_0$) of the response can be trusted, according to the demand that φ_s should remain ''slow.''

A. Internal modes in ESR

The static component of magnetization $\vec{m}$, according to Eq. (3), is directed along the Ox axis. Let us assume that the pumping rf field is parallel to Oz, then the intensity of the ESR signal is proportional to $S^{zz}(0,\omega)$ and is determined by the correlator of m_z. It is easy to see that only the first term in m_z, according to Eq. (3), contributes to $S^{zz}(0,\omega)$ at nonzero frequencies [the last term in Eq. (3) does not depend on φ_s and thus yields the delta function in ω, and the contribution from the second term just vanishes because at $q=0$ the corresponding form factor $f(q)$ in Eq. (18) is zero]. Thus, the significant term in m_z is proportional to $\sin^2\theta_s\dot{\varphi}_s$, and $\dot{\varphi}_s$, according to Eq. (9), is proportional to $\hat{p}_\varphi - \hbar S$, where $\hat{p}_\varphi = -i\hbar\,\partial/\partial\varphi_s$ is the operator of the canonical momentum conjugate to φ_s. Again, $\hbar S$ yields $\delta(\omega)$, so that the only contribution at nonzero ω comes from p_φ. Typical plots of the ESR response depending on frequency for $S=\frac{5}{2}$ are shown in Fig. 2; one can see that the transitions between 0^+ and 0^- soliton levels lead to a pronounced peak with a maximum located well below the antiferromagnetic resonance frequency ω_0. Since the levels 0^+ and 0^- have different minima in their P dependencies, the position of peaks in the ESR response at positive and negative ω is also different. When the temperature increases, peaks shift towards ω_0, but still keep their shape with a clearly pronounced maximum. Thus we expect that this effect can be really observable experimentally in TMMC, where at $H=H_c$ the three-dimensional ordering temperature $T_N \simeq 3$ K, i.e., about $0.15E_0$.

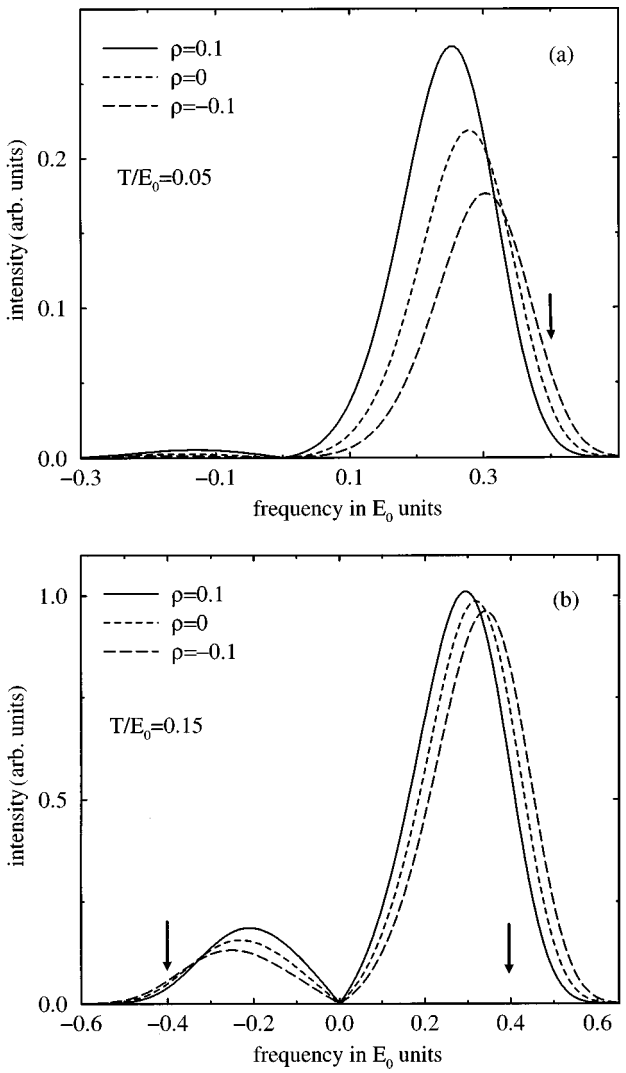

FIG. 2. Plots of $S^{zz}(0,\omega)$ (this quantity determines the intensity of the ESR signal) for $S=\frac{5}{2}$ and different values of the parameter $\rho = 1 - H^2/H_c^2$: (a) $T=0.05E_0$; (b) $T=0.15E_0$. Arrows show the positions of the boundary of the continuous magnon spectrum at $H=H_c$.

B. Internal modes in INS

In neutron experiments, it is usually possible to measure either the longitudinal (with respect to the magnetic field) DSF component $S^{\parallel} = S^{xx}(q,\omega)$, or the transverse one $S^{\perp} = S^{yy}(q,\omega) + S^{zz}(q,\omega)$, with q close to the Bragg wave vector Q_B. In TMMC, both those components exhibit the presence of the soliton central peak.[14] In the transverse DSF the dominating contribution comes from S^{yy} (which corresponds to the contribution of flips of the direction of the antiferromagnetism vector $\vec{l}$ along the easy axis Oy), and S^{yy} is insensitive to the effects of internal modes because l_y does not depend on φ_s; that is why we will be interested only in the longitudinal component S^{xx} determined by the correlator of l_x. Figure 3 shows several typical plots of

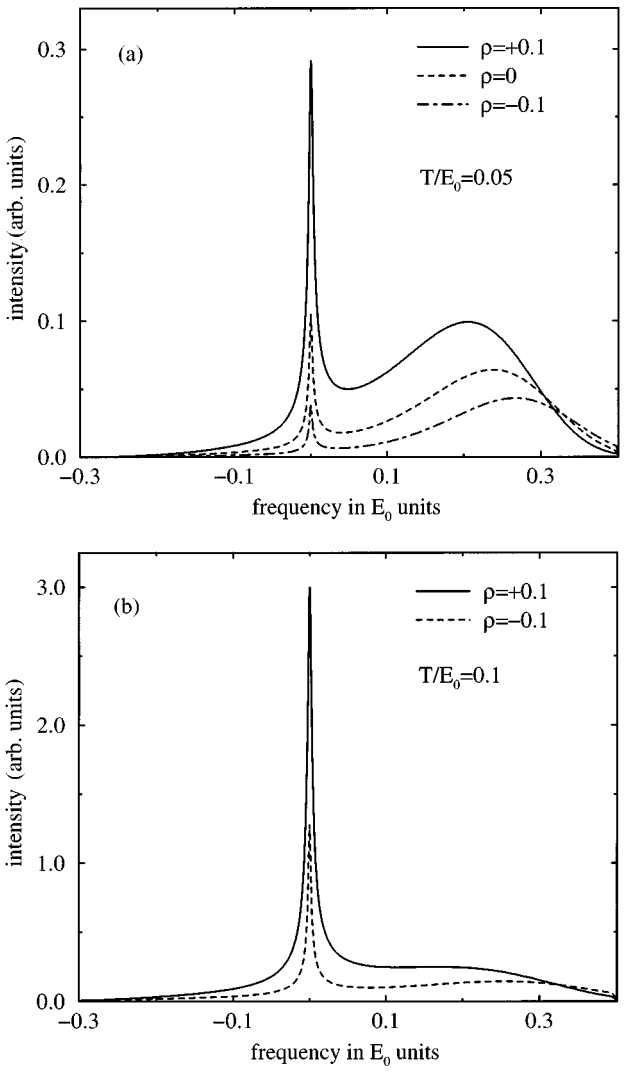

FIG. 3. Plots of the longitudinal DSF $S^{xx}(Q_B,\omega)$ for $S=\frac{5}{2}$ and different values of the parameter $\rho=1-H^2/H_c^2$: (a) $T=0.05E_0$; (b) $T=0.1E_0$.

$S^{xx}(Q_B,\omega)$ for different values of the field and temperature [actually, we have also calculated $S^{xx}(q,\omega)$ for a few values of q close to Q_B, but the resulting curves exhibit very weak q dependence, so we restrict ourselves to presenting only plots for $q=Q_B$]. One can see that the most significant manifestation of internal soliton modes is a nonzero width of the central peak (CP) at $q=Q_B$ (recall that in the standard ideal-gas calculation[6] without taking into account internal degrees of freedom the CP width for the longitudinal component is proportional to $|q-Q_B|$). However, it should be mentioned that the effects of soliton-magnon and soliton-soliton scattering, which we do not consider here, also lead to a nonzero CP width at $q=Q_B$,[32] and therefore it may be problematic to separate those two contributions experimentally. The additional peak at nonzero frequency is also present in S^{xx}, but with increasing temperature it quickly gets smeared by the tails of the dominating central peak [see Fig. 3(b)], and in TMMC at $H\approx H_c$ for $T\geqslant T_N\simeq 0.15E_0$ this peak should be almost completely suppressed.

VI. SUMMARY

We consider the problem of soliton dynamics in a 1D ''almost-classical'' spin-S easy-plane antiferromagnet in strong external magnetic field H, taking into account internal degrees of freedom of solitons. For this purpose, we use the effective Lagrangian approach, which is valid for H close to a certain critical value $H_c\simeq(H_eH_a)^{1/2}$ (where H_e and H_a are the exchange and anisotropy fields, respectively) and allows one to reduce the original continuum field problem to the problem with only two degrees of freedom: one is the soliton coordinate and describes its translational motion, and the other one is the internal angle of out-of-plane deviation. We show that quantum effects of tunneling between two energetically equivalent kink states lead to level splitting for all values of S; the usual selection rule,[19,20] which prohibits the tunneling for half-integer S, is lifted due to the strong coupling between internal and translational modes. It is predicted that this internal mode can be detected in TMMC $[(CD_3)_4NMnCl_3]$ by means of the electron spin resonance or inelastic neutron scattering technique; we also show that ESR is a preferable method because the corresponding resonance peak is much more pronounced compared to that in the INS response.

ACKNOWLEDGMENTS

The authors are grateful to V. G. Bar'yakhtar, H.-J. Mikeska, and G. M. Wysin for stimulating discussions. This work was partially supported by the grant 2.4/27 ''Tunnel'' from the Ukrainian Ministry of Science and Technology.

[1] J. A. Krumhansl and J. R. Schrieffer, Phys. Rev. B **11**, 3535 (1975).
[2] H.-J. Mikeska, J. Phys. C **11**, L29 (1978).
[3] J. K. Kjems and M. Steiner, Phys. Rev. Lett. **41**, 1137 (1978).
[4] H.-J. Mikeska and M. Steiner, Adv. Phys. **40**, 191 (1991).
[5] B. A. Ivanov and A. K. Kolezhuk, Low Temp. Phys. **21**, 255 (1995).
[6] H.-J. Mikeska, J. Phys. C **13**, 2913 (1980).
[7] J. P. Boucher and J. P. Renard, Phys. Rev. Lett. **45**, 486 (1980).
[8] I. Harada, K. Sasaki, and H. Shiba, Solid State Commun. **40**, 29 (1981).
[9] N. Flüggen and H.-J. Mikeska, Solid State Commun. **48**, 293 (1983).
[10] L. P. Regnault, J. P. Boucher, J. Rossat-Mignod, J. P. Renard, J. Bouillot, and W. G. Stirling, J. Phys. C **15**, 1261 (1982).
[11] J. P. Boucher, L. P. Regnault, A. S. T. Pires, J. Rossat-Mignod, Y. Henry, J. Bouillot, W. G. Stirling, and J. P. Renard, in *Magnetic Excitations and Fluctuations*, edited by S. W. Lovesey, U. Bolucani, F. Borsa, and V. Tognetti (Springer, Berlin, 1984), p. 6.
[12] M. E. Gouvea and A. S. T. Pires, Phys. Rev. B **34**, 306 (1986).
[13] G. Wysin, A. R. Bishop, and J. Oitmaa, J. Phys. C **19**, 221 (1986).

[14] J. P. Boucher, L. P. Regnault, R. Pynn, J. Bouilot, and J. P. Renard, Europhys. Lett. **1**, 415 (1986).
[15] B. V. Costa and A. S. T. Pires, Solid State Commun. **56**, 769 (1985).
[16] B. A. Ivanov, A. K. Kolezhuk, and G. K. Oksyuk, Europhys. Lett. **14**, 151 (1991).
[17] B. A. Ivanov and A. K. Kolezhuk, Fiz. Nizk. Temp. **17**, 343 (1991) [Sov. J. Low Temp. Phys. **17**, 177 (1991)].
[18] B. A. Ivanov and A. K. Kolezhuk, Phys. Rev. Lett. **74**, 1859 (1995).
[19] B. A. Ivanov and A. K. Kolezhuk, Low Temp. Phys. **21**, 760 (1995).
[20] B. A. Ivanov and A. K. Kolezhuk, Zh. Eksp. Teor. Fiz. **110**, 2183 (1996) [JETP **83**, 1202 (1996)].
[21] J.-P. Boucher, G. Rius, and Y. Henry, Europhys. Lett. **4**, 1073 (1987).
[22] I. V. Bar'yakhtar and B. A. Ivanov, Fiz. Nizk. Temp. **5**, 759 (1979) [Sov. J. Low Temp. Phys. **5**, 361 (1979)]; Solid State Commun. **34**, 545 (1980).
[23] A. F. Andreev and V. I. Marchenko, Usp. Fiz. Nauk **130**, 39 (1980) [Sov. Phys. Usp. **23**, 21 (1980)].
[24] I. Affleck, Nucl. Phys. B **257**, 397 (1985).
[25] F. D. M. Haldane, J. Appl. Phys. **57**, 3359 (1985).
[26] E. V. Gomonai, B. A. Ivanov, V. A. L'vov, and G. K. Oksyuk, Zh. Eksp. Teor. Fiz. **97**, 307 (1990) [Sov. Phys. JETP **70**, 174 (1990)].
[27] R. F. Dashen, B. Hasslacher, and A. Neveu, Phys. Rev. D **11**, 3424 (1975).
[28] K. Maki, Phys. Rev. B **24**, 3991 (1981).
[29] H.-J. Mikeska, Phys. Rev. B **26**, 5213 (1982).
[30] K. Sasaki, J. Phys. Soc. Jpn. **53**, 2872 (1984).
[31] J. R. Currie, J. A. Krumhansl, A. R. Bishop, and S. E. Trullinger, Phys. Rev. B **22**, 477 (1980).
[32] K. Sasaki and K. Maki, Phys. Rev. B **35**, 257 (1987).